# Numerical investigation on the temperature sensing based on the θ-shaped microfiber resonator

JIAYU XU[a], YIPING XU[a,*], LIYONG REN[b], SHUAI SUN[a], TIANXU JIA[a], LEI ZHANG[a], JIANTING XIAO[a], BINGCHUAN WANG[a], CHENGJU MA[c], SHUBO CHENG[a], FANG CHEN[a], FENG SONG[a,d]

[a]*School of Physics and Optoelectronic Engineering, Yangtze University, Jingzhou 434023, China*

[b]*School of Physics & Information Technology, Shaanxi Normal University, Xi'an 710119, China*

[c]*School of Science, Xi'an Shiyou University, Xi'an 710065, China*

[d]*School of Physics, Nankai University, Tianjin 300071, China*

In this paper, we propose a temperature sensor based on the θ-shaped microfiber resonator. The numerical researched results indicate that the temperature sensing sensitivity of the resonator is closely related to the microfiber diameter and the external refractive index (ERI), while it has little dependence on other parameters. As the microfiber diameter is 1 μm, it reaches the peak value of 2.09 pm/℃. Additionally, as the ERI increases, it improves gradually, then decreases sharply. When the ERI locates at 1.25 to 1.28, it keeps a constant value of about 2.8 pm/℃.

(Received June 23, 2019; accepted August 18, 2020)

*Keywords:* Microfiber, Microfiber resonator, Temperature sensing

## 1. Introduction

As the basic component of industrial development, sensors are often applied and equipped in different systems [1,2], which well meet the requirements of data collection [3,4], fault detection [5-7], etc. In order to satisfy the demand and application of temperature detection in various fields such as medicine, industry and aviation [8-10], different types of temperature sensors have emerged. The main types are thermocouples, thermistors, resistance temperature detectors and IC temperature sensors. They are suitable for different applications and have different characteristics. Thermocouple temperature sensors are self-powered, without excitation, wide range of operating temperature. Thermistor temperature sensors usually achieve high accuracy within a limited temperature range. Resistance temperature detectors of Platinum have high precision, high stability, wide temperature range, and they are suitable for kinds of high precision measurement. The IC temperature sensors have good output characteristics about accurate temperature. Although these temperature sensors have many advantages, they still have some shortcomings that we can't overcome at moment. For example, the output voltage of the thermocouples in measuring temperature is very small, which requires high-precision amplification. In addition, they are sensitive to external noise. The bare resistance temperature detectors have higher thermal stability and slower response to temperature change. Platinum costs more money.

Compared with common temperature sensors, microfiber resonators are compact and simple in structure, have large evanescent field, low loss, easy to manufacture, low cost, low light loss through sharp bending, and good compatibility with traditional optical fibers [11-14], and so on, which have attracted more and more attention. In addition, they are also widely used in optical signal processing, optical filter, wavelength multiplexer, laser and other active devices [15-22].

Typical microfiber resonators include loops, knots, coils and other structures, which have been widely studied [23-29].

In this paper, we propose a temperature sensor based on the θ-shaped microfiber resonator. The propagating characteristics of the light field in the θ-shaped microfiber resonator is analyzed systematically and the theoretical expression about the reflection light field versus the input light field is also given. The temperature sensing principle of the microfiber resonator is analyzed deeply as well. Then, numerical investigation about the temperature sensing sensitivity of the θ-shaped microfiber resonator under different parameters is carried out thoroughly. The researched results indicate that the microfiber diameter making up of the resonator has significant impact on the temperature sensing sensitivity of the resonator. When the microfiber diameter is 1 μm, the temperature sensing sensitivity of the microfiber resonator arrives at the peak value. The external refractive index also has great influence on the temperature sensing sensitivity of the θ-shaped microfiber resonator. When the external refractive index ranges from 1.25 to 1.28, it almost keeps a constant value of 2.8 pm/ºC. However, other parameters, such as coupling coefficients, coupling loss coefficients, the upper arm, the bridge arm, the lower arm, have negligible influence on the sensitivity. This researched consequence will provide some theoretical evidence for the application of the microfiber resonator in the temperature sensing field.

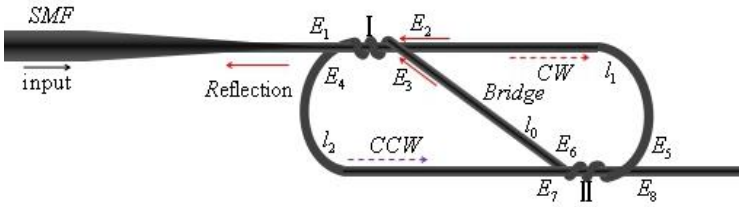


*Fig. 1. Schematic diagram of the θ-shaped microfiber resonator (CW: clockwise direction; CCW: counterclockwise direction)*

## 2. Theoretical model of the θ-shaped microfiber resonator and its temperature sensing principle

The schematic diagram of the θ-shaped microfiber resonator is given in Fig. 1. The whole structure of the resonator is made up of a microfiber. An elliptical cavity is divided by a microfiber bridge into shape of the character "θ". The light field propagating in the resonator can be described as: The input light field $E_1$ injected at the single mode fiber (SMF) splits into $E_2$ and $E_3$ at the coupling area I, $E_2$ propagates along the upper arm $l_1$ and converts into $E_5$, $E_5$ splits at the coupling area II into $E_6$ and $E_7$, $E_7$ propagates along the lower arm $l_2$ and converts into $E_4$, $E_6$ propagates along the bridge arm $l_o$ and converts into $E_3$, this propagating path forms the clockwise direction. Moreover, $E_3$ splits at the coupling area I into $E_1$ and $E_4$, $E_4$ propagates along the lower arm $l_2$ and converts into $E_7$, $E_7$ splits at the coupling area II into $E_8$ and $E_5$, $E_5$ propagates along the upper arm $l_1$ and converts into $E_2$, $E_2$ splits at the coupling area I into $E_1$ and $E_4$; in addition, $E_3$ from $E_1$ or $E_4$ propagates along the bridge arm $l_o$ and converts into $E_6$, $E_6$ splits at the coupling area II into $E_8$ and $E_5$, this propagating path forms the counterclockwise direction. The theory of the θ-shaped microfiber resonator can be developed by combining the theory of ring resonators [30-33] with that of directional couplers [34-36]. For simplicity, we assume that the microfiber, which comprises the θ-shaped microfiber resonator, has the excellent diameter uniformity and surface smoothness, as well as negligible propagation loss [37]. Also, we ignore the bend losses of the θ-shaped microfiber resonator due to the small diameter of the microfiber.

The electric fields of 8 ports can be correlated by coupling mode equation:

$$\begin{pmatrix} E_{2c} \\ E_{3cc} \end{pmatrix} = \left(\sqrt{1-\gamma_1}\right)\begin{pmatrix} \sqrt{1-k_1} & j\sqrt{k_1} \\ j\sqrt{k_1} & \sqrt{1-k_1} \end{pmatrix}\begin{pmatrix} E_{1c} \\ E_{4c} \end{pmatrix}$$
$$E_{5c} = \exp\left(j\beta l_1\right)E_{2c}$$
$$E_{4c} = \exp\left(j\beta l_2\right)E_{7c}$$
$$\begin{pmatrix} E_{6c} \\ E_{7c} \end{pmatrix} = \left(\sqrt{1-\gamma_2}\right)\begin{pmatrix} \sqrt{1-k_2} & j\sqrt{k_2} \\ j\sqrt{k_2} & \sqrt{1-k_2} \end{pmatrix}\begin{pmatrix} E_{5c} \\ E_{8c} \end{pmatrix} \quad (1)$$

$$\begin{pmatrix} E_{1cc} \\ E_{4cc} \end{pmatrix} = \left(\sqrt{1-\gamma_1}\right)\begin{pmatrix} \sqrt{1-k_1} & j\sqrt{k_1} \\ j\sqrt{k_1} & \sqrt{1-k_1} \end{pmatrix}\begin{pmatrix} E_{2cc} \\ E_{3c} \end{pmatrix}$$
$$E_{2cc} = \exp\left(j\beta l_1\right)E_{5cc}$$
$$E_{7cc} = \exp\left(j\beta l_2\right)E_{4cc}$$
$$\begin{pmatrix} E_{5cc} \\ E_{8cc} \end{pmatrix} = \left(\sqrt{1-\gamma_2}\right)\begin{pmatrix} \sqrt{1-k_2} & j\sqrt{k_2} \\ j\sqrt{k_2} & \sqrt{1-k_2} \end{pmatrix}\begin{pmatrix} E_{6cc} \\ E_{7cc} \end{pmatrix} \quad (2)$$

where $k_1$ and $k_2$ are the coupling coefficients, $\gamma_1$ and $\gamma_2$ are the coupling loss coefficients of the coupling area I and the coupling area II, respectively. $\beta$ is the propagation constant given in Ref. [38]. $l_1$ and $l_2$ are the lengths of the upper arm (port 2-5), and the lower arm (port 7-4) of the resonator, respectively. The subscripts *c* and *cc* represent the light fields propagating in clockwise direction and counterclockwise directions, respectively. The above two parts are combined by microfiber bridge:

$$\begin{cases} E_{6cc} = \exp\left(j\beta l_0\right)E_{3cc} \\ E_{3c} = \exp\left(j\beta l_0\right)E_{6c} \end{cases} \quad (3)$$

$l_0$ is the length of microfiber bridge (port 3-6). $L = l_1 + l_2$ is the length of the main chamber of the θ-shaped microfiber resonator. For simplicity, assuming $k_1 = k_2 = k$, $\gamma_1 = \gamma_2 = \gamma$. the reflection of port 1 can be solved by formula (1) - (3):

$$r = E_{1cc} \Big/ E_{1c}$$
$$= 2j\exp\left[j\beta\left(l_1 + l_0\right)\right]\cdot\left(1-\gamma\right)^{1/2}k^{1/2}\times$$
$$\left\{\frac{\left(1-\gamma\right)^2\left(1-k\right)^2\exp\left(j\beta L\right)}{\left[1+\left(1-\gamma\right)k\exp\left(j\beta L\right)\right]^2} + \frac{\left(1-\gamma\right)\left(1-k\right)}{1+\left(1-\gamma\right)k\exp\left(j\beta L\right)}\right\} \quad (4)$$

Thus, the reflection amplitude can be calculated by $R=|r|^2$. Equation (4) indicates that the reflection spectrum of the θ-shaped microfiber resonator is highly dependent on the coupling efficiency *k* and the coupling loss $\gamma$.

In addition, as we all know that the refractive index of the fiber is related to the wavelength of the light propagating in it, the temperature of the fiber and the strain stressed in the fiber. The dependent relationship of the fiber refractive index on the three elements can be expressed as follows[39]:

$$n\left(\lambda, T, \varepsilon\right) = n\left(\lambda, T\right)\left[1 + C_T\left(T - T_0\right) + C_Z\varepsilon\right] \quad (5)$$

where $C_T = \frac{1}{n\left(\lambda, T_0\right)}\frac{\partial n}{\partial T}$ and $C_z = \frac{1}{n\left(\lambda, T_0\right)}\frac{\partial n}{\partial \varepsilon}$ are the temperature coefficient and the strain coefficient of the fiber refractive index, respectively.

So, when we change the temperature of the medium around the θ-shaped microfiber resonator, the refractive index of the microfiber constituting the resonator will also change owing to the thermo-optical effect. Because we don't consider the influence of the strain, the strain coefficient in Eq. (5) can be ignored. Furthermore, due to the temperature coefficient of the fiber material is small, when the temperature variation of the fiber is not too large, the fiber index refractive is also very small. At the vicinity of 1550 nm wavelength, it can be expressed as

$$\Delta n = 0.811\times10^{-5}\Delta T \quad (6)$$

Therefore, under this conditions Eq. (5) can be simplified as

$$n\left(\Delta T\right) = n\left(T_0\right)\left[1 + 0.811\times10^{-5}\Delta T\right] \quad (7)$$

$n\left(T_0\right)$ is the refractive index of the fiber at the room temperature, which is set as 1.45, $T_0$ is the room temperature, $\Delta T = T - T_0$ is the temperature difference between the given temperature and the room temperature.

### 3. Numerical simulation and discussion

In order to study the temperature sensing characteristics of the θ-shaped microfiber resonator, we assume the input light field $E_1 = 1$, the other parameters of the resonator are set as: $k = 0.8$, $\gamma = 0.1$, $\triangle T = 0$℃, $n_1 = 1.45 \times (1 + 0.811 \times 10^{-5} \triangle T)$, $n_2 = 1$, $d = 1 \times 10^{-6}$ m, $l_o = 1000 \times 10^{-6}$ m, $l_1 = 4000 \times 10^{-6}$ m, $l_2 = 4000 \times 10^{-6}$ m. Using Eq. (4), we can simulate the variation of the reflection spectrum of the resonator under different outside temperatures. Fig. 2 (a) gives that one of the resonant wavelengths of the reflection spectrum shifts with the variation of the outside temperature. It can be seen that as the outside temperature increases from 25℃ to 45℃ at an interval of 5℃, the resonant wavelength takes place a red shift. Furthermore, we extract the resonant wavelengths under the outside temperatures of 25℃, 30℃, 35℃, 40℃ and 45℃. The corresponding relationship between the resonant wavelengths and the outside temperatures is given in Fig. 2 (b) .The linear fitting is also given in this figure. One can see that the resonant wavelength of the θ-shaped microfiber resonator nearly increases linearly with the increasing of the outside temperature. The calculated temperature sensing sensitivity of the resonator is about 2.09 pm/ºC.

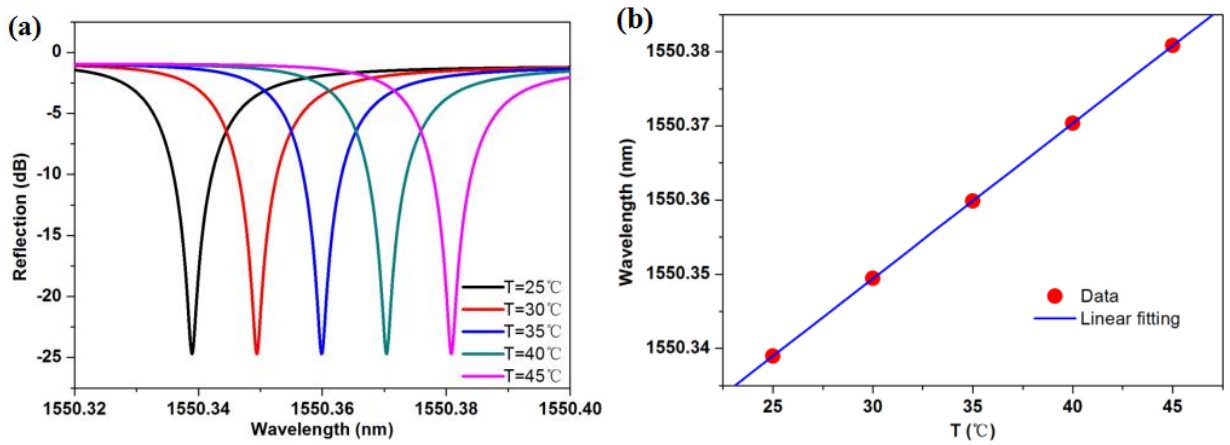


*Fig. 2. (a)Reflection spectra of the θ-shaped microfiber resonator under different outside temperatures.(b)Dependence of the resonant wavelength of the θ-shaped microfiber resonator on different outside temperatures (color online)*

In order to investigate the influence of different parameters (microfiber diameter $d$, external index refractive $n_2$, coupling coefficient $k$, coupling loss coefficient $\gamma$, the upper arm $l_1$, the bridge arm $l_o$, the lower arm $l_2$, etc.) on the temperature sensing sensitivity of the resonator, we research the changes in the relationship between sensitivity and these parameters via numerical simulation method.

Firstly, we investigate the dependence of the temperature sensing sensitivity of the resonator on the microfiber diameter $d$. Assuming the input light field $E_1 = 1$, and other parameters of the resonator are set as: $k = 0.8$, $\gamma = 0.1$, $n_1 = 1.45 \times (1 + 0.811 \times 10^{-5} \triangle T)$, $n_2 = 1$, $l_o = 1000 \times 10^{-6}$ m, $l_1 = 4000 \times 10^{-6}$ m, $l_2 = 4000 \times 10^{-6}$ m. Using Eq. (4) and assuming the outside temperature of the microfiber resonator increases from 25ºC to 45ºC at an interval of 5ºC, we simulate the dependence of the reflection spectrum of the resonator at a fixed microfiber diameter $d$ on the increasing outside temperature. Meanwhile, the corresponding temperature sensing sensitivity of the resonator at the fixed microfiber diameter is calculated from the spectral diagram. As we change the microfiber diameter $d$, the obtained temperature sensing sensitivity is also varied. The changing relationship between the temperature sensing sensitivity of the microfiber resonator and the microfiber diameter $d$ is given in Fig. 3. It can be seen that the temperature sensing sensitivity is zero, when the microfiber diameter is less than 0.4 μm, it enhances sharply as the microfiber diameter increases from 0.4 μm

to 1 μm, but it decreases gradually as the microfiber diameter increases continually. The maximum temperature sensing sensitivity is about 2.09 pm/ºC, when the microfiber diameter is 1 μm.

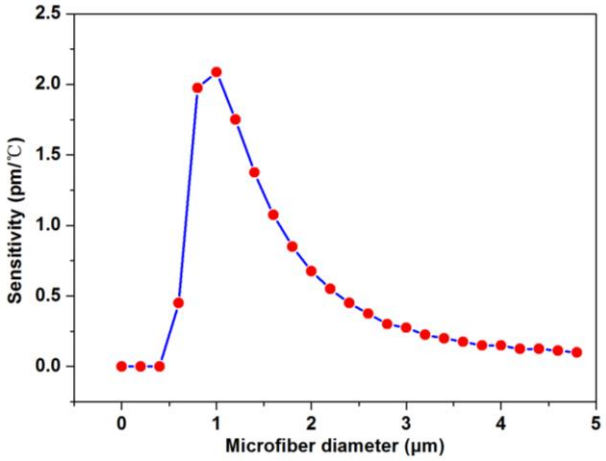


*Fig. 3. Dependence of the temperature sensing sensitivity of the θ-shaped microfiber resonator on the microfiber diameter d (color online)*

The reason for this phenomenon is that when the microfiber diameter $d$ decreases to less than 0.2 μm, the light lunched into the microfiber nearly cannot pass through it. When the microfiber diameter decreases to 0.4 μm, more than 90% power will be lost, and only 10% power will pass through the microfiber. Then, the sensitivity of the waveguide will become extremely tiny. When the diameter increases to more than 0.4 μm, not only does the evanescent field around the microfiber become strong, but also more light can be propagated. So, the sensitivity increases suddenly. However, when the diameter increases to over 1 μm, the evanescent field around the microfiber will become weak gradually [11,40]. Therefore, the sensitivity decreases slowly.

Then, we investigate the influence of the external refractive index $n_2$ on the temperature sensing sensitivity of the θ-shaped microfiber resonator. Similarly, assuming the input light field $E_1 = 1$, and other parameters of the resonator are set as: $k = 0.8$, $\gamma = 0.1$, $n_1 = 1.45 \times (1 + 0.811 \times 10^{-5}\triangle T)$, $d = 1 \times 10^{-6}$ m, $l_o = 1000 \times 10^{-6}$ m, $l_1 = 4000 \times 10^{-6}$ m, $l_2 = 4000 \times 10^{-6}$ m. Using Eq. (4) and assuming the outside temperature of the microfiber resonator increases from 25ºC to 45ºC at an interval of 5ºC, we simulate the dependence of the reflection spectrum of the resonator at a fixed external refractive index $n_2$ on the increasing outside temperature. Meanwhile, the corresponding temperature sensing sensitivity of the resonator at the fixed external refractive index is calculated from the spectral diagram. As the external refractive index varies, the temperature sensing sensitivity of the microfiber resonator is also changed. The dependent relationship between the temperature sensing sensitivity and the external refractive index is given in Fig. 4. One can see that when the external refractive index increases from 1.00 to 1.25, the temperature sensing sensitivity of the θ-shaped microfiber resonator also enhances gradually. Then, it almost keeps a constant value of 2.8 pm/ºC, when the external refractive index locates at 1.25 to 1.28. But, it decreases sharply as the external refractive index exceeds 1.28.

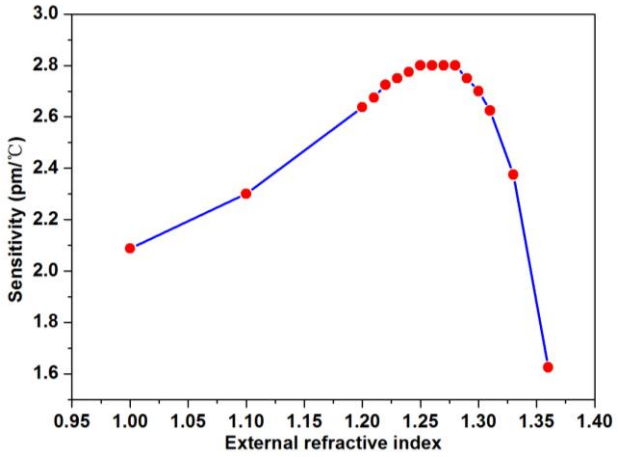


*Fig. 4. Dependence of the temperature sensing sensitivity of the θ-shaped microfiber resonator on the external refractive index (color online)*

Subsequently, we investigate the influence of the coupling coefficient $k$ on the temperature sensing sensitivity of the θ-shaped microfiber resonator. Likewise, assuming the input light field $E_1 = 1$, the other parameters of the resonator are set as: $\gamma = 0.1$, $n_1 = 1.45 \times (1 + 0.811 \times 10^{-5}\triangle T)$, $n_2 = 1$, $d = 1 \times 10^{-6}$ m, $l_o = 1000 \times 10^{-6}$ m, $l_1 = 4000 \times 10^{-6}$ m, $l_2 = 4000 \times 10^{-6}$ m. Using Eq. (4) and assuming the outside temperature of the microfiber resonator increases from 25ºC to 45ºC at an interval of 5ºC, we simulate the dependence of the reflection

spectrum of the resonator at a fixed coupling coefficient on the increasing outside temperature. Meanwhile, the corresponding temperature sensing sensitivity of the resonator at the fixed coupling coefficient is calculated from the spectral diagram. As the coupling coefficient varies, the corresponding temperature sensing sensitivity of the microfiber resonator is also calculated. The dependent relationship between the temperature sensing sensitivity and the coupling coefficient is given in Fig. 5. It can be seen easily that the coupling coefficient has little impact on the temperature sensing sensitivity of the microfiber resonator. Furthermore, we also investigate the influence of the coupling loss coefficient $\gamma$, the upper arm $l_1$, the bridge arm $l_o$, the lower arm $l_2$, etc. on the temperature sensing sensitivity of the θ-shaped microfiber resonator. The obtained results indicate that these parameters also have negligible effect on the temperature sensing sensitivity of the resonator.

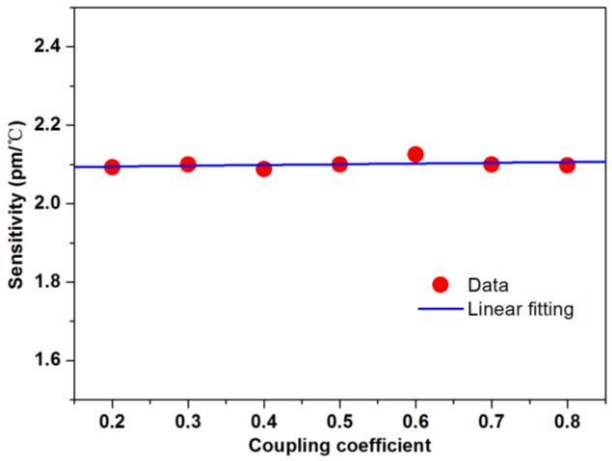


*Fig. 5. Dependence of the temperature sensing sensitivity of the θ-shaped microfiber resonator on the coupling coefficient (color online)*

The main reason is that the evanescent field surrounding the surface of the microfiber can effect the propagating mode in the microfiber, which leads to the shift of the transmission spectrum of the microfiber resonator. So the sensing sensitivity of the microfiber resonator is closely related to the evanescent field surrounding the surface of the microfiber. These parameters, such as coupling coefficient $k$, coupling loss coefficient $\gamma$, the upper arm $l_1$, the bridge arm $l_o$, the lower arm $l_2$, have no influence on the evanescent field, so they also have no influence on the sensing sensitivity.

## 4. Conclusion

In this paper, the θ-shaped microfiber resonator is proposed to be used as a temperature sensing device. Firstly, the propagating behavior of the light field in the θ-shaped microfiber resonator is described systematically. The temperature sensing principle of the microfiber resonator is also analyzed deeply. Then, we theoretically investigate the dependent relationship between the temperature sensing sensitivity of the θ-shaped microfiber resonator and its some parameters, such as microfiber diameter $d$, external refractive index $n_2$, coupling coefficient $k$, coupling loss coefficient $\gamma$, the upper arm $l_1$, the bridge arm $l_o$, the lower arm $l_2$, etc. The researched results reveal that the microfiber diameter $d$ has significant impact on the temperature sensing sensitivity of the resonator. When the range of the microfiber diameter $d$ changes from 0.4 μm to 1 μm，the sensitivity enhances remarkably with the increasing of the microfiber diameter. But, the sensitivity decreases gradually when the microfiber diameter $d$ exceeds 1 μm. Thus, the temperature sensing sensitivity of the microfiber resonator reaches the peak value, as the microfiber diameter $d$ is 1 μm. The external refractive index $n_2$ also has great influence on the temperature sensing sensitivity of the θ-shaped microfiber resonator. When the external refractive index increases from 1.00 to 1.25, the temperature sensing sensitivity of the resonator also enhances gradually. Then, it almost keeps a constant value of 2.8 pm/ºC, when the external refractive index locates at 1.25 to 1.28. But, it decreases sharply as the external refractive index exceeds 1.28. Subsequently, we investigate the dependence of the temperature sensing sensitivity of the resonator on other parameters one by one. The obtained results indicate that these elements have little impact on the sensitivity. This researched consequences will provide some theoretical evidence for the application of the microfiber resonator in the temperature sensing field.

**Acknowledgements**

This work was supported in part by the National Natural Science Foundation of China under Grant Nos. 61605018, 61275149, and 61535015, the Hubei Natural Science Foundation of China under Grant No. 2016CFC767, the Doctoral Scientific Research Startup Foundation of Yangtze University under Grant No. 801080010128, and the Open Research Fund of State Key Laboratory of Transient Optics and Photonics under Grant No. SKLST201612.

## References

[1] J. Vitola, F. Pozo, D. A. Tibaduiza, M. Anaya, Sensors **17**, 417 (2017).

[2] F. Garramiola, J. del Olmo, J. Poza, P. Madina, G. Almandoz, Sensors **18**(5), 1543 (2018).

[3] Y. Zhang, S. He, J. Chen, IEEE/ACM Trans. Netw. **24**(3), 1632 (2016).

[4] H. Chen, B. Jiang, W. Chen, H. Yi, IEEE Trans. Ind. Electron. **66**(6), 4716-4725 (2019).

[5] I. Jlassi, J. O. Estima, S. K. El Khil, N. M. Bellaaj, A. J. M. Cardoso, IEEE Trans. Ind. Appl. **53**(3), 2894 (2017).

[6] H. Chen, B. Jiang, N. Lu, IEEE Trans. Intell. Transp. Syst. **20**(6), 2198 (2019).

[7] H. Chen, B. Jiang, IEEE Transactions on Intelligent Transportation Systems **21**(2), 450 (2019).

[8] M. Fajkus, J. Nedoma, R. Martinek, V. Vasinek, H. Nazeran, P. Siska, Sensors **17**(1), 111 (2017).

[9] R. Fan, Z. Z. Mu, J. Li, J. Phys. Chem. Solids **129**, 307 (2019).

[10] V. R. Mamidi, S. Kamineni, L. N. S. P. Ravinuthala, V. Thumu, V. R. Pachava, Fiber Integr. Opt. **33**(4), 325 (2014).

[11] L. M. Tong, M. Sumetsky, Subwavelength and Nanometer Diameter Optical Fibers, first ed., Zhejiang University Press, Springer, 2009.

[12] Y. P. Xu, L. Y. Ren, J. Liang, C. J. Ma, Y. L. Wang, N. N. Cheng, E. S. Qu, Opt. Commun. **321**, 157 (2014).

[13] L. M. Xiao, T. A. Birks, Opt. Lett. **36**(7), 1098 (2011).

[14] Z. L. Xu, Q. Z. Sun, B. R. Li, Y. Y. Luo, W. G. Lu, D. M. Liu, P. P. Shum, L. Zhang, Opt. Express, **23**(5), 6662 (2015).

[15] X. S. Jiang, Y. Chen, G. Vienne, L. M. Tong, Opt. Lett. **32**(12), 1710 (2007).

[16] Y. H. Chen, Y. Wu, Y. J. Rao, Opt. Commun. **283**(14), 2953 (2010).

[17] Y. P. Xu, L. Y. Ren, C. J. Ma, X. D. Kong, K. L. Ren, Opt. Eng. **55**(12), 126111 (2016).

[18] Y. P. Xu, L. Y. Ren, C. J. Ma, X. D. Kong, K. L. Ren, F. Song, J. Opt. **46**(4), 420 (2017).

[19] Y. P. Xu, L. Y. Ren, J. Liang, C. J. Ma, Y. L. Wang, X. D. Kong, X. Lin, J. Appl. Phys. **118**(7), 073105 (2015).

[20] Y. P. Xu, L. Y. Ren, Y. L. Wang, X. D. Kong, J. Liang, K. L. Ren, X. Lin, Opt. Commun. **350**, 148 (2015).

[21] Y. D. Cui, X. M. Liu, Photon. Res. **7**(4), 423 (2019).

[22] Y. D. Cui, F. F. Lu, X. M. Liu, Sci. Rep. **7**, 400080 (2017).

[23] M. Sumetsky, Y. Dulashko, J. M. Fini, A. Hale, Appl. Phys. Lett. **86**, 161108 (2005).

[24] X. S. Jiang, Q. Yang, G. Vienne, Y. H. Li, L. M. Tong, J. J. Zhang, L. L. Hu, Appl. Phys. Lett. **89**, 143513 (2006).

[25] F. Xu, G. Brambilla, IEEE Photon. Technol. Lett. **19**, 1481 (2007).

[26] C. J. Ma, L. Y. Ren, Y. P. Xu, Y. L. Wang, H. Zhou, H. W. Fu, J. Wen, Appl. Opt. **54**(18), 5619 (2015).

[27] Y. P. Xu, L. Y. Ren, C. J. Ma, X. D. Kong, K. L. Ren, Appl. Opt. **55**(30), 8612 (2016).

[28]Z. L. Xu, Y. Y. Luo, Q. Z. Sun, C. B. Mou, Y. Li, P. P. Shum, D. M. Liu, Optica **4**(8), 945 (2017).

[29] Z. L. Xu, Q. Z. Sun, Y. Y. Luo, P. P. Shum, D. M. Liu, IEEE Photon. Technol. Lett. **30**, 479 (2018).

[30] L. F. Stokes, M. Chodorow, H. J. Shaw, Opt. Lett. **7**(6), 288 (1982).

[31] C. K. Madsen, G. Lenz, IEEE Photon.Technol. Lett. **10**, 994 (1998).

[32] G. T. Paloczi, Y. Huang, A. Yariv, Electron. Lett. **39**, 1650 (2003).

[33] O. Schwelb, J. Light. Technol. **22**, 1380 (2004).

[34] A. W. Snyder, J. D. Love, Optical Waveguide Theory, Chapman & Hall, London, U.K., 1983.
[35] R. B. Smith, J. Opt. Soc. Amer. **66**, 882 (1976).
[36] K. Morishita, T. Yamaguchi, J. Light. Technol. **19**, 732 (2001).
[37] M. Sumetsky, Y. Dulashko, J. M. Fini, A. Hale, D. J. DiGiovanni, J. Light. Technol. **24**, 242 (2006).
[38] M. Sumetsky, Opt. Lett. **31**(7), 3577 (2006).
[39] J. J. Carr, S. L. Saikkonen, D. H. Williams, Fiber Integrated Opt. **9**, 393 (1990).
[40] C. J. Ma, L. Y. Ren, W. G. Guo, H. W. Fu, Y. P. Xu, Y. G. Liu, J. Wen, Appl. Opt. **56**(14), 3984 (2017).

*Corresponding author: ypxu@yangtzeu.edu.cn